Title: Targeting KRAS-mutant stomach/colorectal tumours by disrupting the ERK2-p53 complex

Authors: Xiang Wang[1,#], Qing Xie[1,#], Yan Ji[2], Jiayan Shen[1], Changxu Wang[1], Xu Jiang[1], Zizhuo Chen[1], Yongfeng Zhang[1], Xiangyin Kong[1], Jian Ding[3], Jing-Yu Lang[1,*]

Affiliations:

[1]The CAS Key Laboratory of Tissue Microenvironment and Tumor,

[2]Bioinformatics Core,

Shanghai Institute of Nutrition and Health, Shanghai Institutes for Biological Sciences, University of Chinese Academy of Sciences, Chinese Academy of Sciences, Shanghai, 200031, China.

[3]The State Key Laboratory of Drug Research, Shanghai Institute of *Materia Medica*, Chinese Academy of Sciences, Shanghai, 201203, China.

#These authors contributed equally to this work.

*Correspondence to: jylang@sibs.ac.cn (J.Y.L.).

ABSTRACT

KRAS is widely mutated in human cancers, resulting in nearly unchecked tumour proliferation and metastasis. No therapies have been developed for targeting KRAS-mutant tumours. Herein, we observed that KRAS-mutant stomach/colorectal tumour cells were hypersensitive to the MEK1/2 kinase inhibitor trametinib, which elicits strong apoptotic responses. Genome-wide screening revealed that *TP53* is critical for executing trametinib-induced apoptosis of KRAS-mutant tumours, as validated by *TP53* knockout and rescue experiments. Mechanistically, p53 physically associates with phosphorylated ERK2 in the presence of mutant KRAS, which inactivates p53 by preventing the recruitment of p300/CBP. Trametinib disrupts the p53-ERK2 complex by inhibiting ERK2 phosphorylation, allowing the recruitment of p300/CBP to acetylate p53 protein; acetylated p53 activates PUMA transcription and thereby promotes the apoptosis of KRAS-mutant tumours. Our study unveils an important role of the ERK2-p53 axis and provides a potential therapeutic strategy for treating KRAS-mutant cancer via ERK2 inhibition.

Keywords: KRAS, p53, ERK2, Trametinib, Stomach/colorectal cancer.

Running title: ERK2 preferentially binds with p53 in KRAS-mutant stomach/colorectal cancer.

INTRODUCTION

RAS proteins, including HRAS, NRAS, KRAS4A and KRAS4B, act as central regulators of numerous receptor tyrosine kinase (RTK) signalling pathways[1-3]. In response to extracellular stimuli, RAS proteins are switched from an inactive GDP-bound state to an active GTP-bound state by recruiting guanine nucleotide exchange factors (GEFs), thereby activating the downstream RAF/MEK/ERK, PI3K-mTOR and RALGDS cascades. The members of the RTK/RAS/RAF/MEK pathway are frequently altered in human cancers, enabling tumours to grow unchecked and metastasize[4]. For example, KRAS, together with NRAS and HRAS, is mutated in pancreatic (63.6%), colorectal (37.7%), lung (31.8%), uterine (20%) and stomach (16.4%) adenocarcinomas[5,6]. BRAF is deregulated in approximately 50-60% of melanoma and thyroid adenocarcinomas, while MAP2K1 and MAP2K2, which encode MEK1/2 proteins, are mutated in approximately 4-6% of melanomas. Although RAS proteins play a causal and dominant role in human cancers, it is widely accepted that they are undruggable due to the lack of an accessible site for chemical inhibitors[7]. Newly developed $KRAS^{G12C}$-specific covalent inhibitors exhibit favourable antitumour activity in preclinical settings, accounting for 18.4% of total KRAS mutations at glycine 12[5], but have no effects on other $KRAS^{G12}$ mutants[8,9]. In general, the development of therapies that directly target RAS for patient use largely remains an unmet goal[4,7,10].

Instead of directly targeting RAS proteins, research focus on the downstream effectors of RAS have been productive. BRAF kinase inhibitors, including vemurafenib, dabrafenib and encorafenib, are approved for treating BRAF-mutant melanoma, achieving remarkable clinical responses[11-13]. When tumours develop acquired resistance to BRAF kinase inhibitors, MEK1/2 kinase inhibitors such as trametinib can be applied as either a single agent or combined with BRAF kinase inhibitors[14-17]. Unfortunately, BRAF and MEK1/2 kinase inhibitors only have moderate inhibitory effects in KRAS-mutant lung and pancreatic cancers due to cytostatic responses[17-19]. Thus, it is of great value to develop a strategy for inducing the apoptosis of RAS-mutant tumour cells.

In this study, we observed that stomach/colorectal tumours harbouring RAS mutations are hypersensitive to MEK1/2 inhibition, which increases apoptosis. Using genome-wide knockout screening and functional validation, we discovered that p53 is responsible for executing trametinib-induced apoptosis of KRAS-mutant stomach/colorectal tumour cells. p53 is selectively recruited by phosphorylated ERK2 stimulated by mutant KRAS; this results in p53 inactivation by preventing the recruitment of p300/CBP. Trametinib, a reversible MEK1/2 kinase inhibitor[20], strongly disrupts the ERK2-p53 protein complex by inhibiting ERK2 phosphorylation at threonine 185/tyrosine 187 and promotes the acetylation of p53 protein at lysine 381 and 382 sites by

recruiting p300/CBP, thereby activating p53-mediated *PUMA* transcription. Collectively, our study reveals an important role of the ERK2-p53 complex in maintaining the survival of KRAS-mutant stomach/colorectal tumour cells and provides a potential therapeutic strategy for eliminating these tumours by disrupting the ERK2-p53 interaction.

RESULTS

KRAS-mutant stomach/colorectal cancer cells are hypersensitive to MEK1/2 kinase inhibitors, which induce apoptotic responses.

To evaluate the sensitivity of RAS-mutant tumour cells to MEK1/2 inhibition, we collected the viability data of 771 human cancer cell lines treated with the MEK1/2 inhibitor trametinib from the Genomics of Drug Sensitivity in Cancer database[21]. Trametinib is a potent and reversible MEK1/2 kinase inhibitor that strongly inhibits the phosphorylation of the MEK1/2 effector ERK1/2[19,20]. Data analysis revealed that both the half maximal inhibitory concentration (IC_{50}) and area under the curve (AUC) of 127 human cancer cell lines harbouring RAS hotspot mutations at glycine 12, glycine 13 and glutamine 61 were significantly lower than those of their wild-type counterparts (both $p<1.62E-07$, Figures 1a and 1b). In agreement with previous reports[17-19], trametinib exhibited moderate inhibitory activity in lung and pancreatic cancer subtypes with median IC_{50} values of 3.79±8.71 μM and 3.77±11.01 μM, respectively. Surprisingly, stomach/colorectal cancer cell lines harbouring RAS mutations were hypersensitive to trametinib (median IC_{50}= 0.3±0.45 μM from a total of 23 tumour lines, $p\leq0.01$), and 9 of them had IC_{50} values less than 36 nM. This observation led us to investigate why these RAS-mutant cell lines are hypersensitive to MEK1/2 inhibition.

To validate these data, we collected seven KRAS mutant stomach/colorectal cancer cell lines and examined their responses to trametinib. Cell viability data showed that trametinib potently reduced the viability of 5 of 7 KRAS-mutant tumour lines with IC_{50} values of 10-30 nM (Figure 1c), supporting the fact that RAS-mutant stomach/colorectal cancer cells are sensitive to MEK1/2 inhibition. By contrast, PLX4032, which targets the KRAS downstream effector BRAF[22], had little or no inhibitory effects in all seven KRAS mutant cancer cell lines tested (Figure 1d)[23]. The KRAS mutation status of seven tested tumour cell lines was validated by Sanger sequencing (Figure 1e)[24].

Flow cytometry analysis revealed that trametinib robustly increased the percentage of cells in sub-G1 phase by approximately 26% in both $KRAS^{G12D}$ mutant AGS and GSU cells after 48 hours of treatment compared that observed in vehicle-treated cells ($p<0.001$), but PLX4032 exerted little or no changes in this subpopulation ($p>0.05$, Figures 1f-1h). This suggests that trametinib induces a strong apoptotic response in KRAS-mutant stomach/colorectal tumour cells. Immunoblotting

data further demonstrated that trametinib treatment stimulated PARP cleavage, a typical signature of apoptosis, in the KRAS-mutant cancer cell lines sensitive to trametinib but failed to do so in two cell lines resistant to trametinib (Figure 1i). Notably, the bioactivity of MEK1/2 was markedly inhibited by trametinib in all of the tested cancer cell lines regardless of drug sensitivity, as indicated by reduced levels of phosphorylated ERK1/2 (Figure 1i)[20]. These data suggest that MEK1/2 inhibition is pivotal for initiating trametinib-induced apoptosis of KRAS-mutant stomach/colorectal tumour cells, which can evade apoptosis to survive.

Genome-wide knockout screening shows that *TP53* is a potential candidate for initiating trametinib-induced apoptosis of KRAS-mutant stomach/colorectal tumour cells.

To explore the mechanism by which trametinib induces the apoptosis of KRAS-mutant cells, we performed a genome-scale CRISPR-Cas9 knockout (GeCKO) screen using $KRAS^{G12D}$ mutant GSU cells (Figure 2a). As described in the Materials and Methods[25], GSU cells were first infected with lentiviruses containing the sgRNA library at a multiplicity of infection (MOI) of 0.4 and then selected for 7 days with puromycin to remove uninfected cells. To achieve 300-fold coverage of sgRNAs, $2\text{-}3\times10^7$ cells were harvested for each group after the treatments were finished. Infected cells were divided into three groups based on the treatment type: direct genomic DNA extraction ($DMSO_{day0}$ group), 14 days of treatment with 0.015% DMSO ($DMSO_{day14}$ group) or 14 days of treatment with 15 nM trametinib ($Trametinib_{day14}$ group). After treatment was discontinued, the genomic DNA of each group was harvested, barcode PCR-amplified and deep-sequenced.

Gene ontology analysis revealed that sgRNAs targeting transcription-, translation- and apoptosis-related genes were significantly enriched in the $Trametinib_{day14}/DMSO_{day14}$ group (FDR <0.05, Figure 2b and Supplementary Table 1). Because apoptosis induction was critical for trametinib-induced cell death, we further investigated sgRNAs that target apoptosis-related genes (GO: 0043065). Using the MAGeCK algorithm[26], we identified that sgRNAs targeting *TP53* and its downstream genes, such as *BAX* and *BBC3/PUMA*, were enriched in the $Trametinib_{day14}/DMSO_{day0}$ group compared with the $DMSO_{day14}/DMSO_{day0}$ group (Figure 2c). Using CRISPR score analysis[27], *TP53*, *BBC3* and *BAX* genes were again positively selected (red curve, Figure 2d). As one of the top selected candidates, the levels of sgRNAs targeting *TP53* gene had increased by 12.6- and 5.9-fold with duplicate hits in the $Trametinib_{day14}/DMSO_{day14}$ group (both FDR < 2.1E-116). We obtained similar results in another round of GeCKO screening using $MAP2K1^{Q56P}$ mutant OCUM1 cells[28,29], in which sgRNAs targeting the *TP53* gene were significantly increased 1.3- and 1.9-fold in the $Trametinib_{day14}/DMSO_{day14}$ group (FDR<0.05, Supplemental Figure 1). The low fold change in sgRNA levels was probably attributed to the slow growth rate of OCUM1 cells (doubling time >72 hours).

Our screening data also revealed that the *KRAS* gene is critical for maintaining the survival of $KRAS^{G12D}$ mutant GSU cells, showing that the levels of sgRNAs targeting the *KRAS* gene were significantly reduced in the $DMSO_{day14}/DMSO_{day0}$ group (blue curve, Figure 2d). Clonogenicity data showed that shKRAS knockdown dramatically reduced the numbers of GSU cells compared to that of cells treated with scramble shRNA ($p<0.001$, Supplemental Figure 2), suggesting that our screening data are reliable. Based on these results, we hypothesize that *TP53* and its downstream genes are responsible for mediating trametinib-induced apoptosis of KRAS-mutant tumour cells.

_TP53_ is critical for executing trametinib-induced apoptosis of KRAS-mutant stomach/colorectal tumour cells _in vitro_.

To validate the role of p53, we selected two independent sgRNAs to deplete the *TP53* gene in $KRAS^{G12D}$ mutant GSU and AGS cells. Cell viability data showed that *TP53* gene knockout significantly rescued the viability of GSU cells treated with trametinib compared to that of sgControl cells ($p<0.001$, Figure 3a). The sgRNA knockout efficiency is shown in the upper panel. Similar results were obtained in another $KRAS^{G12D}$ mutated AGS cell line ($p<0.001$, Figure 3b). Notably, reintroduction of wild-type p53 by a doxycycline-inducible vector greatly restored the sensitivity of *TP53* knockout GSU and AGS cells to trametinib ($p<0.001$), which was comparable to that of sgControl cells (Figure 3c), suggesting it's not an off-target effect. Clonogenicity data also illustrated that *TP53* gene knockout markedly increased the numbers of GSU and AGS cells after trametinib treatment, which was abrogated by re-expressing wild-type p53 (Figures 3d and 3e).

Cytoplasmic and nuclear subfractionation data showed that p53 protein accumulated in the nucleus following trametinib treatment for 2 hours and peaked at 24-48 hours, which in turn triggered Puma expression and PARP cleavage in the same time frame (Figure 3f). Bax expression showed little or no changes during the treatment. To evaluate whether p53 is critical for mediating trametinib-induced apoptosis, we checked the expression of pro-apoptotic proteins in the absence or presence of p53. Immunoblotting data demonstrated that trametinib strongly induced the apoptosis of sgControl GSU cells, as indicated by increased Puma expression and caspase/PARP cleavage (Figure 3g). This phenotype was largely abrogated by knocking out *TP53* but was restored by re-expressing wild-type p53 (Figure 3g). Similar results were obtained in another AGS cell line (Supplemental Figure 3). Thus, *TP53* is a key gene responsible for trametinib-induced apoptosis of KRAS-mutant stomach/colorectal tumour cells.

_TP53_ is critical for trametinib-induced cell death of KRAS-mutant stomach/colorectal tumour xenografts _in vivo_.

We further examined whether the *TP53* gene is crucial for transducing the antitumour activity of trametinib *in vivo*. Tumour xenograft data showed that trametinib potently inhibited the *in vivo* growth of GSU tumour xenografts in athymic mice when orally administered at 3 mg/kg twice per week ($p<0.01$), and this inhibitory effect was largely abolished by *TP53* gene knockout ($p>0.05$, Figure 3h). Re-expression of wild-type p53 significantly improved the sensitivity of TP53 knockout GSU tumour xenografts to trametinib compared with vehicle ($p<0.001$, Figure 3i). Immunochemistry staining data showed that trametinib provoked tumour necrosis in sgControl GSU tumour xenografts (Figure 3j), which is consistent with a previous report[18]. The tumour necrosis phenotype vanished in the *TP53* knockout group but was restored when wild-type p53 was exogenously expressed (Figure 3j).

Due to the poor growth of AGS tumour xenografts in nude mice, we transplanted the xenografts into Rag2/Il2rg double knockout mice that lack T, B and NK cells. Again, the tumour xenograft data reinforced the notion that trametinib significantly reduced the *in vivo* growth of AGS tumour xenografts ($p<0.01$), but this antitumour activity was largely abolished by *TP53* gene knockout ($p>0.05$, Figure 3k). Re-expression of wild-type p53 significantly increased the sensitivity of *TP53* knockout AGS tumour xenografts to trametinib ($p<0.05$, Figure 3l).

Collectively, these results lead us to conclude that *TP53* is a key gene that determines the therapeutic responses of KRAS-mutant stomach/colorectal tumour xenografts to trametinib *in vitro* and *in vivo*.

The _TP53_ mutation occurs in the DNA binding domain (amino acids 245-285) and the null mutation confers intrinsic resistance of KRAS-mutant stomach/colorectal tumour cells to trametinib.

TP53 is the most frequently deregulated gene in human cancers and overlaps with *KRAS* gene mutations in Pan-cancer Atlas tumour samples (co-occurrence, $p<0.001$, Supplemental Figure 4)[5,6]. Therefore, we asked which kinds of *TP53* gene mutations affect the therapeutic responses of KRAS-mutant tumour lines to trametinib. We selected the top 24 most frequent *TP53* mutant forms based on the Cosmic and TCGA databases[30-32] and cloned them into a gene expression vector. The clonogenicity data revealed that point mutations in the p53 DNA binding domain (amino acids 245-285) and nonsense mutations such as $TP53^{R213*}$ efficiently abolished the therapeutic effects of trametinib *in vitro*, while other hotspot mutations such as $TP53^{R175H}$ failed to do so (Figure 3m and Supplemental Figure 5). These data explain why SW480 (homozygous

TP53^{R273C}) and SH-10-TC (heterozygous TP53$^{R273H/P309S}$) cancer cell lines are primarily resistant to trametinib despite the fact they harbour the KRAS^{G12V} mutation (Figures 1c and 1i)[24,33]. Collectively, p53 protein, especially the activity of its DNA binding domain, is critical for mediating trametinib-induced apoptosis of KRAS-mutant stomach/colorectal tumour cells.

p53 protein is predominantly sequestered by ERK2 in KRAS-mutant stomach/colorectal tumour cells.

To explore how p53 interacts with the RAS signalling pathway, we performed a coimmunoprecipitation assay and observed that p53 preferentially bound ERK2 (but not ERK1) and other RAS signalling members in AGS cells, and this interaction was strikingly disrupted by trametinib (Figure 4a). We obtained similar results in KRAS^{G12D} mutant GSU cells (Figure 4b). Due to the absence of an ERK2-specific immunofluorescent antibody, we used an antibody that recognizes ERK1/2 proteins to detect whether p53 and ERK2 colocalized. Immunofluorescent double staining data revealed that the majority of p53 protein was colocalized with ERK1/2 in the cytosol of GSU cells, while trametinib markedly abolished this colocalization and promoted p53 nuclearization (Figure 4c). Using an ERK2-specific immunoblotting antibody, we showed that p53 bound ERK2 (Figure 4d). These results suggest that trametinib modulates p53 bioactivity by regulating ERK2.

Mutant KRAS promotes the formation of the ERK2-p53 complex by phosphorylating ERK2 at the T185 and/or Y187 sites.

Next, we asked whether *KRAS* gene mutations can initiate the formation of the ERK2-p53 complex. Exogenous expression of the KRAS^{G12D} mutant visibly increased the levels of phosphorylated ERK2 (Thr185/Tyr187) (Figure 4e)[34]. Highly phosphorylated endogenous ERK2 protein was observed in all six tested KRAS-mutant tumour cell lines (Figure 1i). More importantly, KRAS^{G12D} and MAP2K1^{Q56P} mutants enhanced the physical association between p53 and ERK2 proteins (Figure 4f). This supports our notion that KRAS mutation is a key event for assembling the ERK2-p53 complex.

To further determine whether ERK2 phosphorylation is required for binding with p53 protein, we generated a series of ERK2 mutants harbouring alanine, aspartic acid or glutamic acid substitutions at threonine 185 and/or tyrosine 187[35]. Mutation substitution data revealed that the ERK2 T185A/Y187F mutant, which mimics dephosphorylated ERK2, completely lost its binding affinity with p53 protein, while the T185D/Y187F, T185A/Y187D and T185D/Y187D mutants that mimic single- or double-phosphorylated ERK2 maintained comparable or better binding

ability with p53 protein than did wild-type ERK2 (Figure 4g). We did not observe a notable protein association between the ERK2 T185E/Y187E mutant and p53 protein compared with that of wild-type ERK2, suggesting that this mutant is not a good phosphomimetic. These data indicate that both threonine 185 and tyrosine 187 phosphorylation are important for forming the ERK2-p53 complex.

These data suggest that the KRAS mutation is a driving source for assembling the ERK2-p53 complex by upregulating ERK2 phosphorylation at T185/Y187.

p53 protein interacts with phosphorylated ERK2 through the N-terminal transactivation domain (TAD).

To determine which p53 protein domain is required for binding with phosphorylated ERK2, we generated a series of p53 domain truncation mutants, as shown in Figure 4h. Domain truncation analysis revealed that the p53 protein lacking the TAD completely lost its binding ability with the ERK2 T185D/Y187D mutant that mimicked double-phosphorylated ERK2, while the p53 ΔCTD mutant exhibited a binding affinity to phosphorylated ERK2 comparable with that of wild-type p53 (Figure 4i). This suggests that the TAD domain of p53 protein is required for interacting with phosphorylated ERK2.

In the literature, chemotherapeutic drugs such as doxorubicin can promote p53 phosphorylation at threonine 55 via ERK2[36]. Immunoblotting data showed that there was little or no detectable signal of p53 phosphorylation in our case, including at threonine 55 and seven another phosphorylation sites located in the TAD (Supplemental Figure 6a). Mutation substitution data also demonstrated that both the p53 T55D and T55A mutants had no influence on the response of GSU cells to trametinib (Supplemental Figure 6b). Thus, these results indicate that p53 probably interacts with ERK2 via the unphosphorylated TAD. Moreover, doxorubicin exhibits poor inhibition on RAS mutant stomach/colorectal cancer cell lines with an average IC_{50} value of 4.82±8.25 μM. These data support our notion that disrupting ERK2-p53 complex rather than inducing ERK2-p53 complex is more critical for executing the apoptosis of KRAS mutant gastrointestinal tumours.

ERK2 inhibition, which mimics trametinib treatment, promotes the apoptosis of KRAS-mutant stomach/colorectal tumour cells by initiating p53-mediated Puma transcription.

To determine whether ERK2 inhibition is critical for killing KRAS-mutant tumour cells, we used shRNA to silence ERK2 as well as ERK1 in both *TP53* wild-type and knockout GSU cells. Clonogenicity data showed that shERK2 knockdown significantly reduced the numbers of

sgControl GSU cells, a response which mimicked that of trametinib treatment ($p<0.001$, Figure 5a). When *TP53* was knocked out, neither shERK2 knockdown nor trametinib reduced cell growth ($p>0.05$, Figure 5a). shERK1 knockdown had little or no effect in both cases, suggesting that this is an ERK2-specific event. Next, we repeated this experiment with two ERK2 kinase inhibitors, AZD0364 and SCH772984[37,38]. Cell viability data showed that both AZD0364 and SCH772984 significantly reduced the viability of $KRAS^{G12D}$ mutant GSU cells, but their inhibitory effects were significantly reduced by *TP53* gene knockout (Figure 5b). Similar to trametinib treatment, both AZD0364 and SCH772984 stabilized p53 protein levels, increased Puma expression and promoted PARP cleavage (Figure 5c). Phosphorylation of the ERK effector p90RSK, which is akin to the inhibitory activity of ERK2 inhibitors[37], declined after AZD0364 and SCH772984 treatment. p21 expression was also decreased after treatment with trametinib or ERK2 inhibitors. Taken together, our data suggest that trametinib induces the apoptosis of KRAS-mutant tumour cells via ERK2 inhibition.

Among the downstream effectors of p53 signalling, Puma, Noxa and Bax are critical for executing apoptosis[39-43]. Immunoblotting data showed that trametinib as well as two ERK2 inhibitors significantly induced Puma protein expression but had little or no impact on Noxa or Bax protein expression (Figure 5c). The qRT-PCR data revealed that both trametinib and the two ERK2 inhibitors induced Puma mRNA expression in a p53-dependent manner (Figures 5d and 5e). RNA interference data showed that shPuma knockdown almost completely restored the viability of GSU cells treated with trametinib when compared with that of scramble cells ($p<0.001$, Figure 5f), suggesting that p53-mediated *PUMA* transcription is critical for trametinib-induced apoptosis of KRAS-mutant tumour cells.

To determine how p53 regulates *PUMA* transcription, we individually cloned two p53 binding sites of the *PUMA* promoter into a pGL3-basic-luciferase vector (Figure 5g, upper panel)[44]. Luciferase expression data revealed that p53 binding site 2 but not binding site 1 responded to trametinib (Figure 5g). When *TP53* was depleted, binding site 2 was also inactivated. This suggests that trametinib provokes *PUMA* transcription by recruiting p53 protein to p53 binding site 2 of the *PUMA* promoter, which is critical for inducing the apoptosis of KRAS-mutant tumour cells.

Trametinib promotes p53 protein acetylation at lysine 382 by recruiting p300/CBP, which is crucial for activating *PUMA* transcription.

Next, we asked how trametinib modulates the transcriptional activity of the p53 protein, which is largely determined by posttranslational modifications, including ubiquitination and acetylation[45,46]. Due to the failure to detect changes in p53 ubiquitination (data not shown), we

asked whether the acetylation modification of p53 protein is critical for initiating *PUMA* transcription[47-49]. To evaluate which acetylation site is critical for p53 transcriptional activity, we constructed a series of p53 mutants harbouring glutamine or arginine substitutions at lysine 120, 370, 372, 373, 381 and 382[45,50,51]; these substitutions mimic acetylated or deacetylated lysine, respectively (Figure 5h, upper panel). After exogenous expression of the p53 mutants in *TP53* knockout GSU cells, the 5KQ, 2KQ and K382Q mutants, but not K120Q or the other mutants, significantly enhanced Puma mRNA expression levels upon trametinib treatment; the levels were the same as or better than those induced by wild-type p53 ($p<0.01$, Figure 5h). Of note, the K382Q mutant itself, which mimics the K382-acetylated form of p53 protein, was sufficient to initiate trametinib-induced *PUMA* transcription. Immunoblotting data confirmed that p53 protein was acetylated at lysine 382 after trametinib treatment in multiple sensitive cancer cell lines, including GSU and AGS, accompanied by Puma expression (Figure 5i). Similar to trametinib, AZD0364 and SCH772984 obviously increased p53 and K382-acetylated p53 protein expression levels (Figures 5c and 5j). As expected, shERK2 but not shERK1 increased the protein expression levels of p53 and K382-acetylated p53 (Figure 5k). To examine whether this increase is a general mechanism for MEK1/2 inhibitors, we selected another five MEK1/2 inhibitors with different chemical structures and observed that they all enhanced the protein expression of total p53 and K382-acetylated p53 (Figure 5l). Thus, our data suggest that MEK1/2 inhibition is pivotal for stimulating trametinib-induced p53 acetylation at lysine 382, which in turn activates *PUMA* transcription.

Next, we asked whether p300/CBP, sharing 96% sequence identity, is the acetyltransferase that modifies trametinib-induced K382 acetylation of p53 protein[45,46,52,53]. Coimmunoprecipitation data revealed that p53 physically associated with ERK2 in the absence of trametinib but preferentially bound p300 in the presence of trametinib; this interaction was accompanied by decreased MDM2 expression (Figures 4a, 4b and 6a). We obtained similar results in another $KRAS^{G12D}$ mutant GSU cell line that lacked MDM2 expression (Figure 6b). Because p300/CBP interacts with the p53 protein through the N-terminal TAD[54], the physical association of the ERK2-p53 complex potentially blocks the recruitment of p300/CBP to the p53 protein by occupying the TAD and thereby preventing the acetylation of the p53 protein. To address this issue further, we selected the p300/CBP-specific inhibitor CPI-637 and examined whether p300/CBP was required to prompt trametinib-induced acetylation of p53 protein at lysine 382. Immunoblotting data showed that CPI-637 treatment greatly decreased the levels of total and acetylated p53 upon trametinib treatment (Figure 6c). Importantly, CPI-637 treatment robustly increased the viability of GSU cells treated with trametinib to levels comparable to *TP53* knockout (Figure 6d). Thus, we

conclude that p300/CBP is critical for acetylating p53 protein at lysine 382, which is a key event for inducing trametinib-mediated apoptosis.

In the literature, p300/CBP can simultaneously acetylate p53 at five lysine sites (370, 372, 373, 381 and 382), which prevents protein degradation by blocking ubiquitination[45,50]. To determine which acetylation site is critical for maintaining p53 protein stability, we transiently transfected p53 wild-type and the indicated mutant forms into 293T cells and observed that the 5KQ and 2KQ mutants had higher protein expression levels than did wild-type p53 (Figure 6e). K382Q and K382R showed little or no changes in their stability compared with that of wild-type p53, suggesting that the acetylation of p53 protein at lysine 381 is important for improving its protein stability. Indeed, we observed that trametinib increased the levels of p53 K381 acetylation in KRAS-mutant cancer cell lines (Figure 6f).

In summary, p53 protein is sequestered by phosphorylated ERK2 in KRAS-mutant stomach/colorectal tumour cells, which prevents its association with p300/CBP; trametinib disrupts the ERK2-p53 complex via inhibition of ERK2 phosphorylation. This allows p53 acetylation at lysine 381 and 382 by p300/CBP, thereby activating p53-mediated *PUMA* transcription and the apoptosis cascade (Figure 6g). Thus, we provide a potential therapeutic strategy for eliminating RAS-dependent cancer by disrupting the ERK2-p53 complex, which is helpful for developing cancer therapies to target diseases with mutant KRAS.

DISCUSSION

In this study, we revealed the existence of the ERK2-p53 protein complex in KRAS-mutant stomach/colorectal tumour cells, which is critical for maintaining tumour sensitivity to MEK1/2 kinase inhibitors. Stomach and colorectal adenocarcinomas frequently present amplified expression of RTK/RAS pathway members, such as *MET*, *FGFR2*, *EGFR* and *KRAS*[6,55], all of which can potentially activate the MEK1/2-ERK2 cascade. To examine this hypothesis, we collected a total of forty-three stomach cancer cell lines and recorded their MEK1/2 phosphorylation levels under serum-free conditions, as shown in Supplemental Figure 7a (lower right panel, grey curve). After screening, we observed that trametinib efficiently decreased the viability of 18 of 43 stomach cancer cell lines with IC_{50} values of 5-100 nM. Upon retrieving data from the CCLE database[24], we identified that stomach cancer cell lines harbouring KRAS (7/8), NRAS (1/1) and MAP2K1 (1/1) mutations, except SH-10-TC (heterozygous $TP53^{R273H/P309S}$), were hypersensitive to trametinib. To our surprise, trametinib exhibited potent inhibitory effects in MET-amplified (4/5) stomach cancer cell lines but not in other RTK-amplified stomach cancer cell lines, with IC_{50} values of 10-50 nM, showing increased levels of Puma and K382-acetylated

p53 protein (Supplemental Figures 7a and 7b). Hs746T, which contains a $TP53^{K319*}$ mutation, is the only tested MET-amplified cell line with no response to trametinib[24]. Re-introduction of wild-type p53 greatly sensitized Hs746T cells to trametinib, which was accompanied by increased Puma expression ($p<0.001$, Supplemental Figures 7c and 7d). These data suggest that MET amplification is another driving factor for assembling the ERK2-p53 complex. Notably, recent clinical trials illustrate that trametinib has potential therapeutic value for treating KRAS-mutant colorectal tumours[56,57]. Therefore, it would be of great value to examine whether trametinib can treat KRAS- and MET-mutant stomach/colorectal tumours in clinical settings.

It is unclear why trametinib exhibited weaker inhibition in KRAS-mutant lung and pancreatic cancers. Unlike the stringent regulation of the RAS/RAF/MEK cascade, over 250 substrates downstream of ERK1/2 have been identified[58,59], which corresponds to profound diversity of ERK2-associated complexes. On the other hand, p53-binding proteins are also highly dynamic and are associated with Bcl-xL protein in normal cells[60,61]. Thus, the assembly of the ERK2-p53 complex is highly selective and predominant in KRAS-mutant stomach/colorectal cancers, whose bioactivity is potentially compensated by other ERK2-associated complexes in different cancer subtypes. More efforts are needed to determine the detailed mechanism in the future.

Notably, the BRAF inhibitor vemurafenib/PLX4032 had no inhibitory effects on any of the seven tested KRAS-mutant stomach/colorectal cancer cells (Figures 1d, 1f-1h). Not surprisingly, PLX4032 did not disrupt the ERK2-p53 complex due to its inability to inhibit ERK2 phosphorylation (Supplemental Figure 8). In the literature, PLX4032 selectively targets mutant but not wild-type BRAF[23], which explains why PLX4032 does not inhibit ERK2 phosphorylation in KRAS-mutant tumour cells.

Finally, ERK reactivation is a key event for cells to develop acquired resistance to BRAF and MEK1/2 kinase inhibitors[14,15,62,63]. In this study, ERK2 kinase inhibitors strongly inhibited the growth of KRAS-mutant stomach/colorectal cancer cells, which was comparable to the activity of trametinib. Thus, therapies directly targeting ERK2 provide a new opportunity for killing KRAS-mutant stomach/colorectal cells with the advantages of circumventing ERK reactivation and reducing the toxicity of ERK1 inhibition.

METHODS

Cell Lines. The gastric cancer cell lines were purchased from Korean Cell Line Bank, RIKEN BRC Cell Bank or JCRB Cell Bank, respectively. Lovo and SW480 cell lines were purchased from the cell bank of Shanghai Institutes for Biological Sciences (Shanghai, China). Cells were cultured in either RPMI 1640 or DMEM/F12 medium with 10% fetal bovine serum (Hyclone) and 1%

penicillin streptomycin (Life Technologies), and were incubated at 37°C with 5% CO_2. All cell lines were recently authenticated with STR assays, keeping as mycoplasma-free.

Reagents. Trametinib, AZD6244 and MG132 were purchased from Selleck Chemicals (Shanghai, China). AZD0364 was purchased from MedChemExpress (MCE) (Shanghai, China). CPI-637 and SCH772984 was purchased from TargetMol. Puromycin, choloroquine, polybrene, NaCl, NaF, Na3VO4, PMSF, Tween 20, sucrose, PEG400, Cremophor® EL, PEG8000 and DMSO were purchased from Sigma-Aldrich (Saint Louis, USA). Thiazolyl blue tetrazolium bromide (MTT) and Tris were purchased from VWR (Radnor, USA). The primary antibodies against phospho-p44/42(ERK1 Thr202/Tyr204, ERK2 Thr185/Tyr187) (#4377, 1:6,000), ERK1/2 (#9102, 1:6,000), acetyl-p53 (Lys382) (#2525,1:2,000), phosphor-p53 (Ser6) (#9285T, 1:1,500), phosphor-p53 (Ser9) (#9288T, 1:1,500), phosphor-p53 (Ser15) (#9286T, 1:1,500), phosphor-p53 (Thr18) (#2529T, 1:1,500), phosphor-p53 (Ser20) (#9287T, 1:1,500), phosphor-p53 (Ser46) (#2521T, 1:1,500), phosphor-p53 (Thr81) (#2676T, 1:1,500), cleaved caspase-3 (#9664, 1:2,000), cleaved caspase-6 (#9761, 1:2,000), cleaved caspase-7 (#8438, 1:2,000), cleaved caspase-9 (#7237, 1:2,000) and cleaved PARP (#5625, 1:1,000) were obtained from Cell Signaling Technology. Primary antibodies against Puma α/β (sc-28226, 1:2,000), Bax (sc-7480, 1:2,000), p53 (sc-126, 1:3,000), p21 (sc-397, 1:3,000), Noxa (sc-56169, 1:1,000), ERK2 (sc-135900, 1:2,000), p300 (sc-48343, 1:3000), lamin B (sc-6216, 1:3,000), HA-probe (sc-7392, 1:2,000) and vinculin (sc-25336, 1:3,000) were obtained from Santa Cruz Biotechnology. Primary antibodies against β-tubulin (ab135209, 1:5,000), phospho-p53 (Thr55) (ab183546, 1:1,500) and acetyl-p53 (K381) (ab61241, 1:3,000) were purchased from Abcam. Primary antibodies against Flag-tag (F3165, 1:3,000) was obtained from Sigma-Aldrich.

Plasmids. Human CRISPR Knockout Pooled Library (GeCKO v2) (#1000000048), LentiCRISPR v2 (#52961), pMD2.G (#12259), pRSV-Rev (#12253) and pMDLg/pRRE (#12251) were purchased from Addgene. The TP53 and ERK2 constructs were obtained from CAS_Key Laboratory of Tissue Microenvironment and Tumor. The $KRAS^{G12D}$ and $MAP2K1^{Q56P}$ mutants were cloned from GSU and OCUM1 cells, respectively, validated by Sanger Sequencing. The DNA sequence of 3× p53 binding site 1 (5'-CTCCTTGCCTTGGGCTAGGCC-3') and 3× p53 binding site 2 (5'-CTGCAAGTCCTGACTTGTCC-3') was individually cloned into a pGL3-basic luciferase vector. TP53 and ERK2 mutant constructs were generated by PCR cloning as mentioned. Primers for generating gene were listed in Supplementary Table 2 and shRNA constructs were listed in Supplementary Table 3.

Cell viability assay. Cells were seeded into 96-well plates at a density of 5,000-6,000/well, and were treated with Chemical at final concentrations of 0.01, 0.03, 0.1, 0.3, 1, 3, and 10 μM on the next day, followed by 72 hours' incubation at 37°C with 5% CO_2. When treatment stopped, cells were then added with 20 μl MTT solution for 4 hours, followed by 12-16 hours' incubation with 50 μl triplex solution (0.012 M HCl, 10% SDS, and 5% isobutanol) before detecting OD570 nm.

Colony formation assay. Cells were plated into 6-well plates at a density of 1,000-3,000/well, and were treated by trametinib or vehicle (0.3% DMSO) at 37°C for two weeks. After treatment stopped, colonies were fixed and stained with a mixture of 6% glutaraldehyde and 0.5% crystal violet for 1 hour. The density of colonies was captured and analyzed by Image J software.

Immunoprecipitation. Cells were lysed on ice with 1× lysis buffer containing 1 mM Na_3VO_4, 1 mM NaF, 1 mM PMSF and protease inhibitor cocktail (Cat.11873580001, Roche). After pre-cleaned, primary antibodies were added to the supernatant of cell lysates and incubated at 4 °C overnight. The protein A/G agarose beads (SC-2003, Santa Cruz) or Dynabeads™ protein G beads (#10004D, Invitrogen) were added into each sample and incubated at 4 °C for 1-2 hours on the next day. The precipitants were washed with 1× lysis buffer for five times, boiled for 10 min and were subjected to immunoblotting.

Quantitative PCR. Total RNA was extracted from cultured cells using Trizol™ reagent, and was reversed into cDNA with PrimerScript™ RT reagent Kit (RR037A). Quantitative PCR was performed with NovoStart SYBR qPCR supermix using ABI-7500 instrument. GAPDH was used as an internal reference to normalize input cDNA. Primers for real time PCR were listed in Supplementary Table 4.

CRISPR/Cas9-mediated knock out. Two annealed sgRNA oligos targeting TP53 gene were cloned into lentiCRISPRv2 vector after digested with BsmBI. Target cells were transiently transfected with sgRNA plasmids using Lipofectamine® 3000, followed by puromycin selection for 3 days to remove uninfected cells. Cells were seeded into 96-well plates at a density of one cell per well, and knockout clones were validated by immunoblotting and Sanger sequencing. sgRNA oligos were listed in Supplementary Table 3.

Immunofluorescence staining. Cells were plated into 24-well plates pre-seated German glass cover slips, and were subjected to trametinib or vehicle (0.3% DMSO) for indicated time. After fixed with 4% formaldehyde, cells were blocked with 3% BSA for 1 hour and incubated with primary antibody at 4 °C overnight. After wash with three times, cells were incubated with Alexa Fluor® 488 or Rhodamine Red™-X labeled secondary antibody (Jackson ImmuoResearch) at

room temperature for 1 hour. DAPI was added into the cells before mounting and cells were imaged with a fluorescence microscope.

Immunohistochemistry staining. After dissecting tumour tissues, samples were fixed with 4% paraformaldehyde at 4°C overnight. Then, tumour samples were stained with haematoxylin and eosin staining (Wuhan Servicebio Technology, China) following standard protocol.

Cytoplasmic and Nuclear Extraction. Cells were first lysed with 800 µl lysis buffer (10 mM HEPES: pH 7.9, 10 mM KCl, 2 mM MgCl, 0.1 mM EDTA, 0.2% NP40) with protease inhibitor (#11697498001, Roche). The supernatant (cytoplasmic fraction) was collected after centrifuged at 13,000 rpm at 4°C for 10 min. After washed twice, the nuclei pellet was further lysed with 250 µl cell lysis buffer (#9803, CST) with protease inhibitor. The nuclear fraction was collected after centrifuged at 13,000 rpm at 4°C for 10 min after sonication. The subfraction samples were subjected to immunoblotting analysis.

Luciferase assay. Cells were transfected with indicated plasmid using electroporation, and pRL-TK was used as an internal control. After cultured for 24 hours, cells were treated with trametinib for another 36 hours. After treatment stopped, relative luciferase units (RLU) were measured using the Dual-Glo Luciferase Assay System (Promega) according to the manufacturer's instructions. RLUs from firefly luciferase signal were normalized by RLUs from Renilla signal.

Flow cytometric analysis. After treated with 100 nM trametinib or 0.3% DMSO for 48 hours, cells were fixed with 1 mL of 70% ice-cold ethanol at 4°C overnight. After washed with 1× PBS, cells were stained with propidium iodide (C1052, Beyotime) at 37°C for 30 min and were analyzed using Beckman Gallios flow cytometry. Data were analyzed using a FlowJo software.

GeCKO library screen. The complete GeCKO library screen procedure was previously described[25]. Briefly, GSU cells were infected with an optimal volume of viruses containing sgRNA library at an MOI of 0.4, and were subjected to puromycin for 7 days to remove uninfected cells. After puromycin selection, 2×10^7 GSU cells were collected as $DMSO_{Day0}$ group and were stored at -80℃. The remaining cells were divided into two groups, followed by 0.015% DMSO ($DMSO_{Day14}$ group) or 15 nM trametinib for another 14 days ($Trametinib_{Day14}$ group). To keep 300-fold sgRNA coverage, 2-3 $\times10^7$ living cells were harvested for each group when treatment stopped. The genomic DNA was extracted with Qiagen Blood & Cell Culture Midi kit, followed by PCR amplification, and was sequenced using Illumina HiSeq 2500 by GENEWIZ (Suzhou, China).

***In vivo* tumour xenograft models.** BALB/c nude mice were purchased from Shanghai SLAC

Laboratory Animal Company. All the experimental procedures were approved by the Institutional Animal Care and Use Committee of Shanghai Institute for Nutrition and Health. Cells were injected subcutaneously in the right flank of each mouse. Mice were divided into different groups based on the average tumour volume of each group, approximately 100-150 mm^3. Trametinib (3 mg/kg), or vehicle (10% PEG400, 10% Cremophor® EL) was orally administrated, twice per week. Doxycycline (1 mg/ml) was added to the drinking water to induce p53 expression. Then tumour was measured twice weekly and tumour volume was calculated by the formula $V= 0.5\times L\times W^2$ (V: volume, L: length, W: width).

Statistical analysis. Data represent means ± SD of 2-3 independent repeats. Statistical significance was determined by Student's *t*-test and different levels of statistical significance were denoted by p-values (*p < 0 .05, **p < 0 .01, ***p <0.001).

Availability of data. The GeCKO library data has been deposited in the NCBI GEO (http://www.ncbi.nlm.nih.gov/geo) under accession number GSE152846. All relevant data supporting the key findings are available from the corresponding author upon reasonable request.

Acknowledgments

This work is financially supported by grants from Chinese Academy of Sciences (QYZDB-SSW-SMC034, XDA12020210), National Natural Science Foundation of China (81322034, 81872890) and National Key R&D Program of China (2016YFC1302400).

Declarations of interests

The authors declare that they have no conflicts of interest.

Acknowledgement

We thank the excellent service of institutional core facilities including Molecular Biology and Biochemistry and laboratory animal technical platforms.

References

1. Kolch, W. Coordinating ERK/MAPK signalling through scaffolds and inhibitors. *Nat Rev Mol Cell Biol* **6**, 827-837 (2005).
2. Malumbres, M. & Barbacid, M. RAS oncogenes: the first 30 years. *Nat Rev Cancer* **3**, 459-465 (2003).
3. Simanshu, D.K., Nissley, D.V. & McCormick, F. RAS Proteins and Their Regulators in Human Disease. *Cell* **170**, 17-33 (2017).
4. Downward, J. Targeting RAS signalling pathways in cancer therapy. *Nat Rev Cancer* **3**, 11-22 (2003).
5. Hoadley, K.A., *et al.* Cell-of-Origin Patterns Dominate the Molecular Classification of 10,000 Tumors from 33 Types of Cancer. *Cell* **173**, 291-304 e296 (2018).
6. Liu, Y., *et al.* Comparative Molecular Analysis of Gastrointestinal Adenocarcinomas. *Cancer Cell* **33**, 721-735 e728 (2018).

7. McCormick, F. Targeting KRAS Directly. *Annu Rev Cancer Biol* **2**, 81-90 (2018).
8. Janes, M.R., *et al.* Targeting KRAS Mutant Cancers with a Covalent G12C-Specific Inhibitor. *Cell* **172**, 578-589 e517 (2018).
9. Ostrem, J.M., Peters, U., Sos, M.L., Wells, J.A. & Shokat, K.M. K-Ras(G12C) inhibitors allosterically control GTP affinity and effector interactions. *Nature* **503**, 548-551 (2013).
10. McCormick, F. KRAS as a Therapeutic Target. *Clin Cancer Res* **21**, 1797-1801 (2015).
11. Flaherty, K.T., *et al.* Inhibition of mutated, activated BRAF in metastatic melanoma. *N Engl J Med* **363**, 809-819 (2010).
12. Chapman, P.B., *et al.* Improved survival with vemurafenib in melanoma with BRAF V600E mutation. *N Engl J Med* **364**, 2507-2516 (2011).
13. Ascierto, P.A., *et al.* Phase II trial (BREAK-2) of the BRAF inhibitor dabrafenib (GSK2118436) in patients with metastatic melanoma. *J Clin Oncol* **31**, 3205-3211 (2013).
14. Little, A.S., Smith, P.D. & Cook, S.J. Mechanisms of acquired resistance to ERK1/2 pathway inhibitors. *Oncogene* **32**, 1207-1215 (2013).
15. Ahronian, L.G., *et al.* Clinical Acquired Resistance to RAF Inhibitor Combinations in BRAF-Mutant Colorectal Cancer through MAPK Pathway Alterations. *Cancer Discov* **5**, 358-367 (2015).
16. Lito, P., Rosen, N. & Solit, D.B. Tumor adaptation and resistance to RAF inhibitors. *Nat Med* **19**, 1401-1409 (2013).
17. Solit, D.B., *et al.* BRAF mutation predicts sensitivity to MEK inhibition. *Nature* **439**, 358-362 (2006).
18. Manchado, E., *et al.* A combinatorial strategy for treating KRAS-mutant lung cancer. *Nature* **534**, 647-651 (2016).
19. Jing, J., *et al.* Comprehensive predictive biomarker analysis for MEK inhibitor GSK1120212. *Mol Cancer Ther* **11**, 720-729 (2012).
20. Gilmartin, A.G., *et al.* GSK1120212 (JTP-74057) is an inhibitor of MEK activity and activation with favorable pharmacokinetic properties for sustained in vivo pathway inhibition. *Clin Cancer Res* **17**, 989-1000 (2011).
21. Yang, W., *et al.* Genomics of Drug Sensitivity in Cancer (GDSC): a resource for therapeutic biomarker discovery in cancer cells. *Nucleic Acids Res* **41**, D955-961 (2013).
22. Bollag, G., *et al.* Vemurafenib: the first drug approved for BRAF-mutant cancer. *Nat Rev Drug Discov* **11**, 873-886 (2012).
23. Joseph, E.W., *et al.* The RAF inhibitor PLX4032 inhibits ERK signaling and tumor cell proliferation in a V600E BRAF-selective manner. *Proc Natl Acad Sci U S A* **107**, 14903-14908 (2010).
24. Barretina, J., *et al.* The Cancer Cell Line Encyclopedia enables predictive modelling of anticancer drug sensitivity. *Nature* **483**, 603-607 (2012).
25. Liu, T., *et al.* MYC predetermines the sensitivity of gastrointestinal cancer to antifolate drugs through regulating TYMS transcription. *EBioMedicine* **48**, 289-300 (2019).
26. Li, W., *et al.* MAGeCK enables robust identification of essential genes from genome-scale CRISPR/Cas9 knockout screens. *Genome Biol* **15**, 554 (2014).
27. Wang, T., *et al.* Identification and characterization of essential genes in the human genome. *Science* **350**, 1096-1101 (2015).
28. Gannon, H.S., *et al.* Identification of an "Exceptional Responder" Cell Line to MEK1 Inhibition: Clinical Implications for MEK-Targeted Therapy. *Mol Cancer Res* **14**, 207-215 (2016).
29. Marks, J.L., *et al.* Novel MEK1 mutation identified by mutational analysis of epidermal growth factor receptor signaling pathway genes in lung adenocarcinoma. *Cancer Res* **68**, 5524-5528 (2008).
30. Gao, J., *et al.* Integrative analysis of complex cancer genomics and clinical profiles using the cBioPortal. *Sci Signal* **6**, pl1 (2013).
31. Cerami, E., *et al.* The cBio cancer genomics portal: an open platform for exploring multidimensional cancer genomics data. *Cancer Discov* **2**, 401-404 (2012).
32. Forbes, S.A., *et al.* COSMIC: somatic cancer genetics at high-resolution. *Nucleic Acids Res* **45**, D777-D783 (2017).
33. Rochette, P.J., Bastien, N., Lavoie, J., Guerin, S.L. & Drouin, R. SW480, a p53 double-mutant cell line retains proficiency for some p53 functions. *J Mol Biol* **352**, 44-57 (2005).
34. Botta, G.P., Reginato, M.J., Reichert, M., Rustgi, A.K. & Lelkes, P.I. Constitutive K-RasG12D activation of ERK2 specifically regulates 3D invasion of human pancreatic cancer cells via MMP-

1. *Mol Cancer Res* **10**, 183-196 (2012).
35. Prowse, C.N., Hagopian, J.C., Cobb, M.H., Ahn, N.G. & Lew, J. Catalytic reaction pathway for the mitogen-activated protein kinase ERK2. *Biochemistry* **39**, 6258-6266 (2000).
36. Yeh, P.Y.*, et al.* Phosphorylation of p53 on Thr55 by ERK2 is necessary for doxorubicin-induced p53 activation and cell death. *Oncogene* **23**, 3580-3588 (2004).
37. Ward, R.A.*, et al.* Discovery of a Potent and Selective Oral Inhibitor of ERK1/2 (AZD0364) That Is Efficacious in Both Monotherapy and Combination Therapy in Models of Nonsmall Cell Lung Cancer (NSCLC). *J Med Chem* **62**, 11004-11018 (2019).
38. Pegram, L.M.*, et al.* Activation loop dynamics are controlled by conformation-selective inhibitors of ERK2. *Proc Natl Acad Sci U S A* **116**, 15463-15468 (2019).
39. Levine, A.J. & Oren, M. The first 30 years of p53: growing ever more complex. *Nat Rev Cancer* **9**, 749-758 (2009).
40. Schuler, M. & Green, D.R. Mechanisms of p53-dependent apoptosis. *Biochem Soc Trans* **29**, 684-688 (2001).
41. Villunger, A.*, et al.* p53- and drug-induced apoptotic responses mediated by BH3-only proteins puma and noxa. *Science* **302**, 1036-1038 (2003).
42. Jeffers, J.R.*, et al.* Puma is an essential mediator of p53-dependent and -independent apoptotic pathways. *Cancer Cell* **4**, 321-328 (2003).
43. Shibue, T.*, et al.* Integral role of Noxa in p53-mediated apoptotic response. *Genes Dev* **17**, 2233-2238 (2003).
44. Yu, J., Zhang, L., Hwang, P.M., Kinzler, K.W. & Vogelstein, B. PUMA induces the rapid apoptosis of colorectal cancer cells. *Mol Cell* **7**, 673-682 (2001).
45. Gu, W. & Roeder, R.G. Activation of p53 sequence-specific DNA binding by acetylation of the p53 C-terminal domain. *Cell* **90**, 595-606 (1997).
46. Yang, X.J. & Seto, E. Lysine acetylation: codified crosstalk with other posttranslational modifications. *Mol Cell* **31**, 449-461 (2008).
47. Brooks, C.L. & Gu, W. Ubiquitination, phosphorylation and acetylation: the molecular basis for p53 regulation. *Curr Opin Cell Biol* **15**, 164-171 (2003).
48. Jeon, B.N.*, et al.* ZNF509S1 downregulates PUMA by inhibiting p53K382 acetylation and p53-DNA binding. *Biochim Biophys Acta Gene Regul Mech* **1860**, 962-972 (2017).
49. Brochier, C.*, et al.* Specific acetylation of p53 by HDAC inhibition prevents DNA damage-induced apoptosis in neurons. *J Neurosci* **33**, 8621-8632 (2013).
50. Sykes, S.M.*, et al.* Acetylation of the p53 DNA-binding domain regulates apoptosis induction. *Mol Cell* **24**, 841-851 (2006).
51. Tang, Y., Luo, J., Zhang, W. & Gu, W. Tip60-dependent acetylation of p53 modulates the decision between cell-cycle arrest and apoptosis. *Mol Cell* **24**, 827-839 (2006).
52. Iyer, N.G.*, et al.* p300 regulates p53-dependent apoptosis after DNA damage in colorectal cancer cells by modulation of PUMA/p21 levels. *Proc Natl Acad Sci U S A* **101**, 7386-7391 (2004).
53. Ito, A.*, et al.* p300/CBP-mediated p53 acetylation is commonly induced by p53-activating agents and inhibited by MDM2. *EMBO J* **20**, 1331-1340 (2001).
54. Ferreon, J.C.*, et al.* Cooperative regulation of p53 by modulation of ternary complex formation with CBP/p300 and HDM2. *Proc Natl Acad Sci U S A* **106**, 6591-6596 (2009).
55. Chia, N.Y. & Tan, P. Molecular classification of gastric cancer. *Ann Oncol* **27**, 763-769 (2016).
56. Wu, C.*, et al.* Phase I Trial of Trametinib with Neoadjuvant Chemoradiation in Patients with Locally Advanced Rectal Cancer. *Clin Cancer Res* (2020).
57. Huijberts, S.*, et al.* Phase I study of lapatinib plus trametinib in patients with KRAS-mutant colorectal, non-small cell lung, and pancreatic cancer. *Cancer Chemother Pharmacol* (2020).
58. Eblen, S.T. Extracellular-Regulated Kinases: Signaling From Ras to ERK Substrates to Control Biological Outcomes. *Adv Cancer Res* **138**, 99-142 (2018).
59. Unal, E.B., Uhlitz, F. & Bluthgen, N. A compendium of ERK targets. *FEBS Lett* **591**, 2607-2615 (2017).
60. Chipuk, J.E.*, et al.* Direct activation of Bax by p53 mediates mitochondrial membrane permeabilization and apoptosis. *Science* **303**, 1010-1014 (2004).
61. Mihara, M.*, et al.* p53 has a direct apoptogenic role at the mitochondria. *Mol Cell* **11**, 577-590 (2003).
62. Komatsu, N., Fujita, Y., Matsuda, M. & Aoki, K. mTORC1 upregulation via ERK-dependent gene

654 expression change confers intrinsic resistance to MEK inhibitors in oncogenic KRas-mutant cancer
655 cells. *Oncogene* **34**, 5607-5616 (2015).
656 63. Liu, F., Yang, X., Geng, M. & Huang, M. Targeting ERK, an Achilles' Heel of the MAPK pathway,
657 in cancer therapy. *Acta Pharm Sin B* **8**, 552-562 (2018).
658

Figure 1

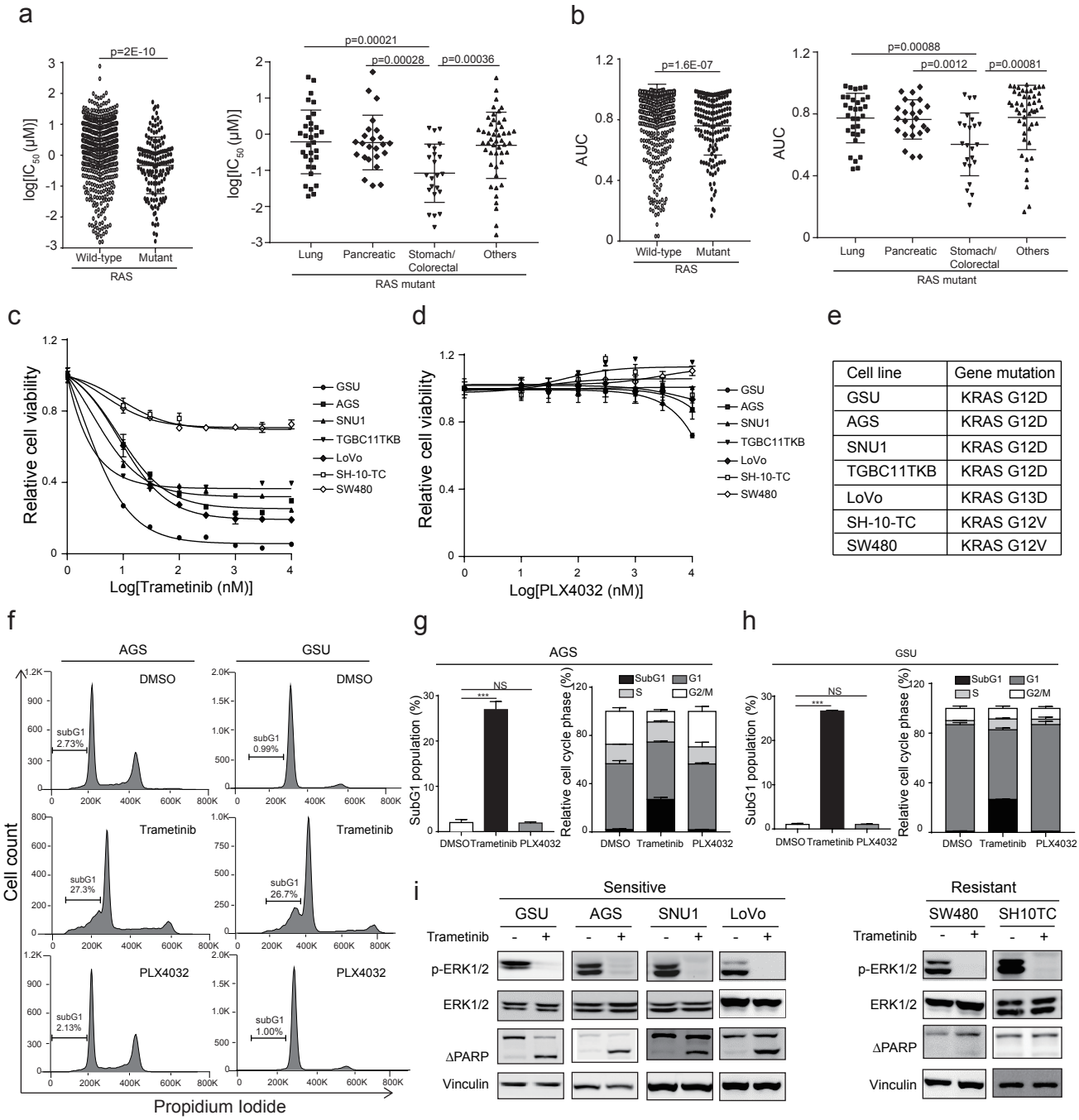

Figure 1. Trametinib potently induces the apoptosis of KRAS-mutant stomach/colorectal cancer cell lines. (a-b) The half maximal inhibitory concentrations (IC_{50}) and area under the curve (AUC) of 771 human cancer cell lines responding to trametinib were obtained from the Genomics of Drug Sensitivity in Cancer database. The statistical significance was calculated by Student's t-test after they were divided into two groups (RAS wild-type, n=623; RAS mutant, n=148). Cancer cell lines harbouring RAS hotspot mutations at glycine 12, glycine 13 and glutamine 61 sites were further divided into four subgroups, including RAS-mutant lung cancer (n=32), RAS-mutant pancreatic cancer (n=24), RAS-mutant stomach/colorectal cancer (n=23) and other RAS-mutant cancers (n=48). Twenty-one cell lines with non-hotspot RAS mutations were excluded. (c) The viability of 7 KRAS-mutant stomach/colorectal cancer cell lines treated with trametinib for 72 hours at the indicated concentrations were determined by an MTT assay. (d) The viability of 7 KRAS-mutant stomach/colorectal cancer cell lines treated with PLX4032 for 72 hours at the indicated concentrations were determined. (e) Sanger sequencing was used to verify the gene mutation status of 7 KRAS-mutant tumour cell lines. (f) GSU and AGS cells were subjected to flow cytometric analysis after treatment with 100 nM trametinib or 100 nM PLX4032 for 48 hours. (g-h) The percentages of GSU and AGS cells in different phases of the cell cycle after trametinib or PLX4032 treatment were calculated. Data represent the means ± SD of three independent experiments. ***p<0.001, Student's t-test. (i) The protein expression levels of p-ERK1/2 (ERK1 Thr202/Tyr204, ERK2 Thr185/Tyr187), ERK1/2 and cleaved PARP in four sensitive and two resistant KRAS mutant cell lines were detected after treatment with 100 nM trametinib for 4 or 48 hours. Vinculin was used as a loading control.

Figure 2

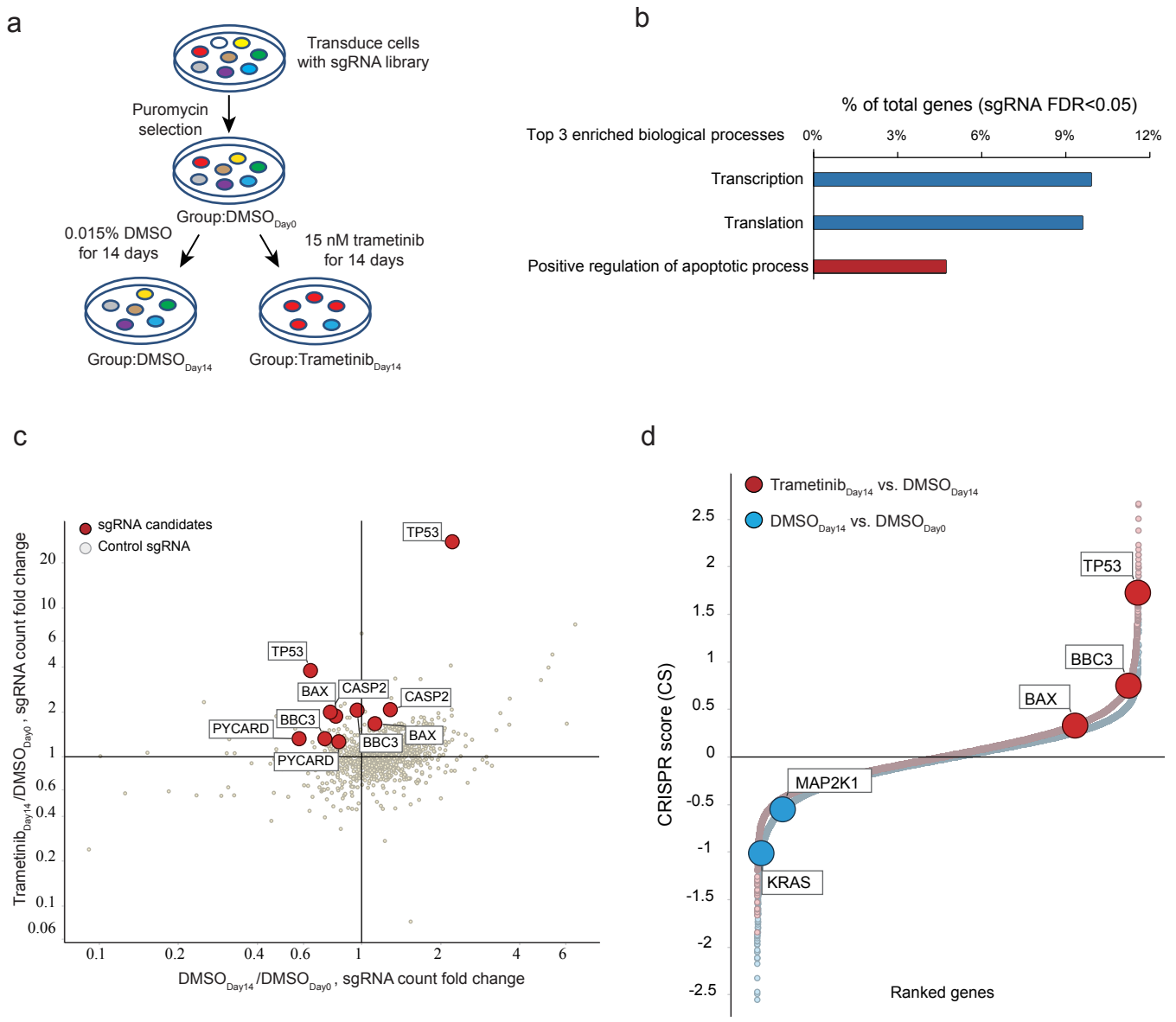

Figure 2. Genome-scale screening reveals that *TP53* is a key gene candidate for executing trametinib-induced apoptosis of KRAS-mutant GSU cells. (a) The working flow chart of the genome-scale CRISPR-Cas9 knockout screen. (b) Gene ontology analysis showed that sgRNAs targeting transcription, translation and positive regulation of the apoptotic process were significantly changed after trametinib treatment compared with after vehicle treatment (FDR <0.05, Fold change >1.35). (c) MAGeCK analysis revealed that sgRNAs targeting *TP53* and downstream genes such as *BBC3*/*PUMA* were enriched in the Trametinib$_{day14}$/DMSO$_{day0}$ vs. DMSO$_{day14}$/DMSO$_{day0}$ group. (d) CRISPR score analysis revealed that *TP53* and *BBC3* were positively selected in the Trametinib$_{day14}$ vs DMSO$_{day14}$ group.

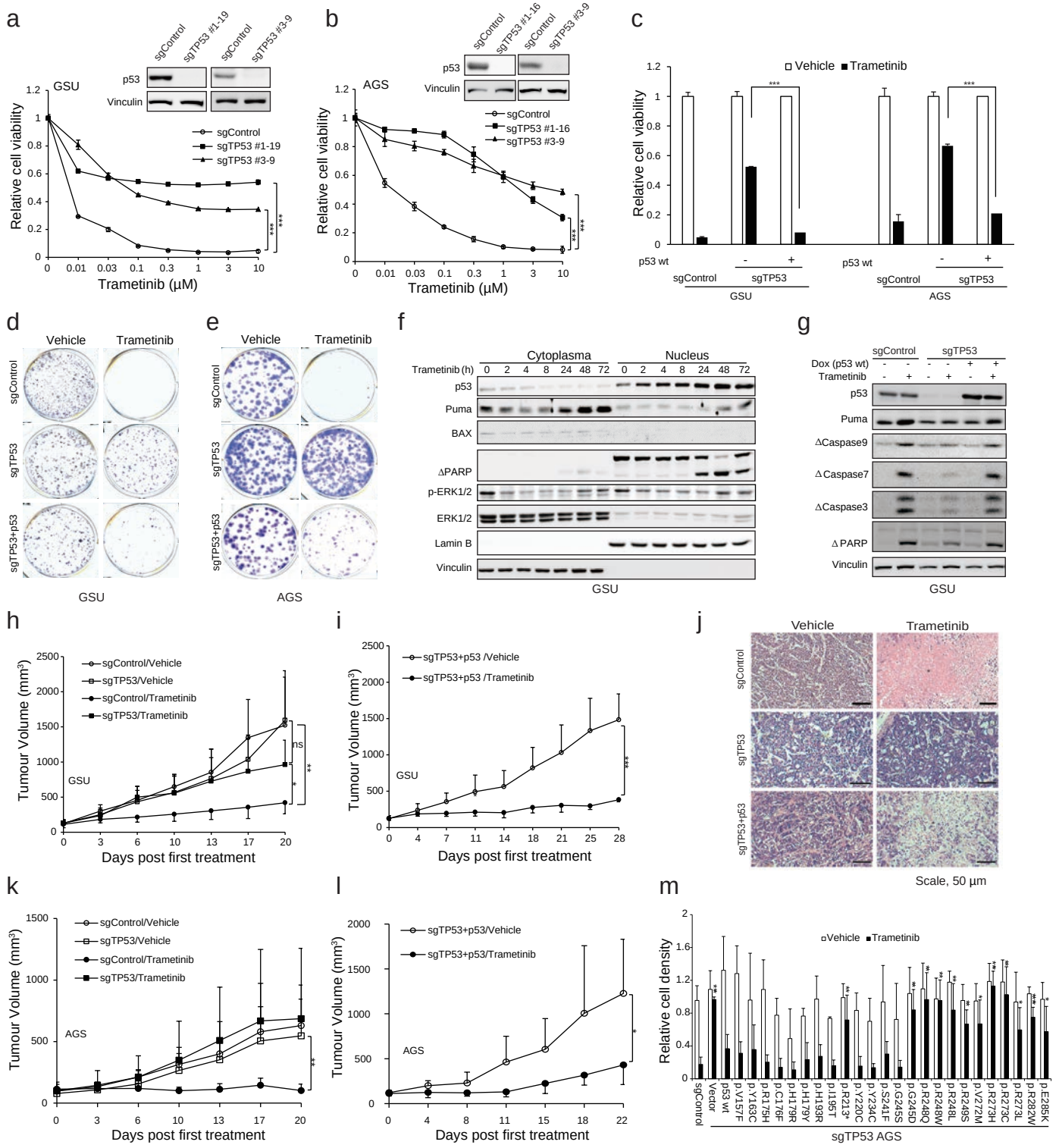

Figure 3. *TP53* is critical for trametinib-induced apoptosis of KRAS-mutant tumour cells. (a) *TP53* gene knockout significantly restored the viability of KRAS-mutant GSU cells. The knockout efficiency of *TP53* gene was shown in the upper panel. (b) *TP53* gene knockout significantly restored the viability of KRAS-mutant AGS cells. The *TP53* gene knockout efficiency was shown in the upper panel. (c) p53 restoration resensitized TP53-knockout cells to trametinib in both the GSU and AGS cell lines. (d-e) *TP53* gene knockout significantly increased clonogenic characteristics of GSU and AGS cells, which was abrogated by re-expression of wild-type p53. (f) Trametinib promoted nuclear accumulation of p53 after treatment 100 nM trametinib for 4 hours, peaked at 24 hours, and robustly induced Puma expression and PARP cleavage at 24 hours. Lamin B was used as a nuclear loading control, while vinculin was used as a cytoplasmic loading control. (g) *TP53* knockout significantly blocked trametinib-induced Puma expression, PARP and caspase cleavage in GSU cells, which was reproduced by re-expressing wild-type p53.Vinculin was used as a loading control. (h) Trametinib markedly reduced the *in vivo* growth of GSU tumour xenografts in nude mice ($p<0.01$), which was overcome by koncking out *TP53* ($p>0.05$). (i) Ectopic of wild-type p53 resensitized sgTP53 GSU tumour xenografts to trametinib in athymic mice ($p<0.001$). (j) Trametinib elicited tumour necrosis of GSU tumour tissue samples as detected by haematoxylin and eosin staining but failed to do so in GSU sgTP53 tumour tissue samples. Tumour necrosis was reproduced by re-expressing wild-type p53. Scale bar, 50 μm. (k) Trametinib markedly reduced the *in vivo* growth of AGS tumour xenografts in Rag2/Il2r double knckout mice ($p<0.01$), but failed to do so in AGS sgTP53 tumour xenografts ($p>0.05$). (l) Ectopic of wild-type p53 restored the sensitivity of AGS sgTP53 tumour xenografts to trametinib ($p<0.05$). (m) The indicated TP53 mutants were stably transfected into TP53 knockout AGS cells, and the clonogenicity of these cells was measured after treatment with 1 nM trametinib for 14 days. Data represent the means ± SD of 3 independent experiments. *$p<0.05$, **$p<0.01$, ***$p<0.001$, by Student's t-test.

Figure 4

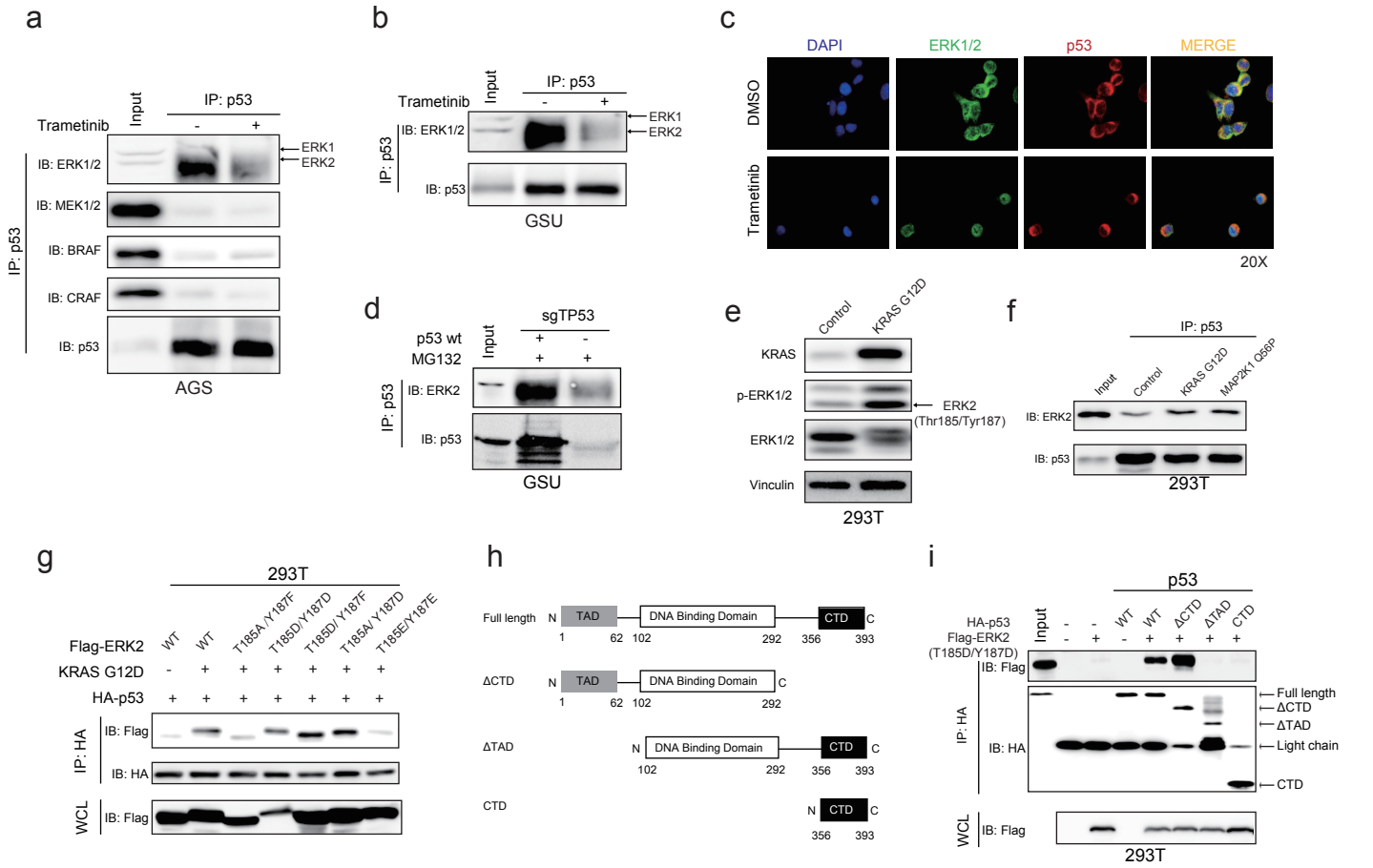

Figure 4. Mutant KRAS promotes the physical interaction between ERK2 and p53 proteins by regulating ERK2 phosphorylation at Thr185 and Tyr187 sites. (a) Coimmunoprecipitation data showed that p53 physically interacted with ERK2 but not ERK1, MEK1/2, BRAF or CRAF proteins in KRAS-mutant AGS cells. The ERK2-p53 complex was largely disrupted by treatment with 1 μM trametinib for 12 hours. (b) p53 physically associated with ERK2 but not ERK1 in KRAS-mutant GSU cells, and this interaction was strongly inhibited by trametinib. (c) Immunofluorescent double staining showed that p53 largely colocalized with ERK1/2 in GSU cells, while trametinib abolished this colocalization and promoted p53 accumulation in the nucleus. (d) Using an ERK2-specific antibody, it was confirmed by coimmunopreicipitation assay that p53 selectively interacted with ERK2 when wild-type p53 was introduced into TP53 knockout GSU cells. (e) Exogenous expression of the $KRAS^{G12D}$ mutant robustly enhanced ERK2 phosphorylation (Thr185/Tyr187) in 293T cells. Vinculin was used as a loading control. (f) Exogenous expression of $KRAS^{G12D}$ and $MAP2K1^{Q56P}$ mutants enhanced the physical interaction between ERK2 and p53. (g) Both Thr185 and Tyr187 sites were critical for ERK2 to interact with p53. The four indicated ERK2 mutants, which mimicked double-, single- and de-phosphorylated ERK2, were transiently transfected into 293T cells and subjected to coimmunoprecipitation assay after culturing for 48 hours. Wild-type p53 in the absence or presence of the $KRAS^{G12D}$ mutant was used as a control. (h-i) The transactivating domain (TAD) of p53 protein is critical for binding with phosphorylated ERK2. Truncated p53 mutants were transiently transfected into 293T cells and were coimmunoprecipitated with the ERK2 T185D/Y187D mutant after culturing for 48 hours. The protein expression of the Flag-ERK2 T185D/Y187D mutant in the whole cell lysate (WCL) was shown at the bottom.

Figure 5

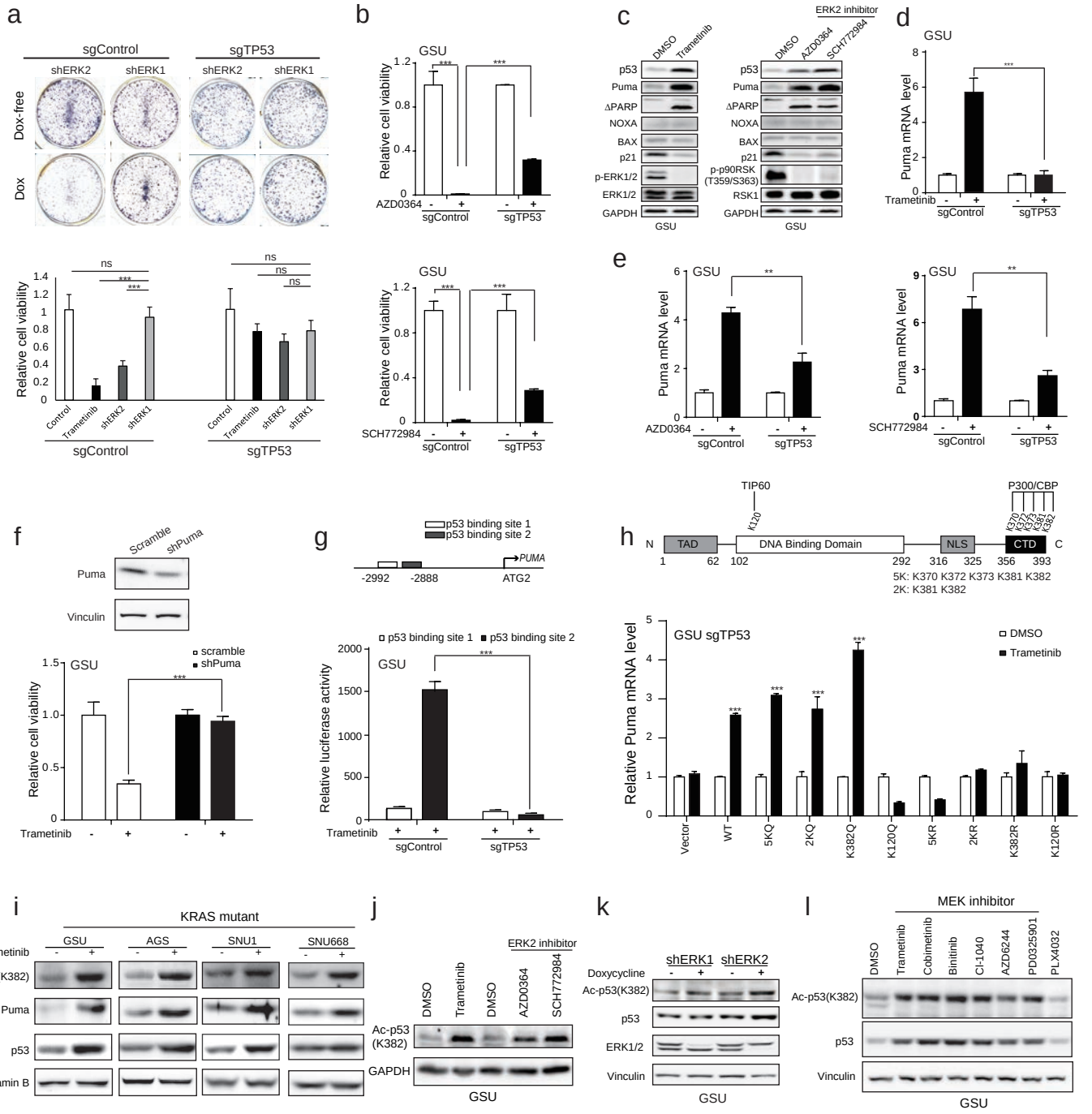

Figure 5. ERK2 inhibition is critical for trametinib-induced apoptosis of KRAS-mutant tumour cells via acetylation of 53 at lysine 382. (a) Knockdown of ERK2 but not ERK1 significantly decreased the colony-forming ability of GSU cells, but this inhibitory effect was abolished by *TP53* gene knockout. 1 nM Trametinib was used as a control. (b)The ERK2 inhibitor AZD0364 and SCH772984 at 1-3 μM potently reduced the viability of GSU sgControl cells but had much less pronounced inhibitory effect in sgTP53 cells. (c) AZD0364 and SCH772984, the effects of which mimic those of trametinib, robustly increased the protein expression of Puma and the cleavage of PARP after treatment for 48 hours but exhibited little or no effect on the expression of Noxa and BAX. The inhibitory effects of AZD0364 and SCH772984 were determined by monitoring the levels of the ERK2 effector phosphorylated p90RSK (Thr359/Ser363). GAPDH was used as a loading control. (d) Trametinib induced Puma mRNA expression in a p53-dependent manner. (e) The ERK2 inhibitor AZD0364 and SCH772984 also elicited Puma mRNA expression in a p53-dependent manner. (f) shPuma robustly abolished the inhibitory effect of trametinib in GSU cells. The shPuma knockdown efficiency was shown in the upper panel. (g) p53 binding site 2 of the *PUMA* promoter is critical for trametinib-induced *PUMA* transcription. (h) The p53 wild-type, 5KQ, 2KQ and K382Q mutants, but not other mutants, significantly promoted the mRNA expression of Puma upon trametinib treatment. 5K indicates the lysines at 370, 372, 373, 381 and 382, while 2K indicates the lysines at 381 and 382. The domain structure of the p53 protein was shown in the upper panel. (i) Trametinib increased the levels of K382 acetylation of p53 protein as well as the expression of Puma protein in multiple KRAS-mutant stomach cancer cell lines. Lamin B was used as a loading control. (j) The ERK2 inhibitor AZD0364 and SCH772984 increased the expresssion of K382-acetylated p53 protein. (k) shERK2 but not shERK1 increased the protein expression of total and K382-acetylated p53 in GSU cells. (l) Trametinib with another five MEK1/2 kinase inhibitors with different chemical structures increased both total p53 and K382-acetylated p53 protein expression, while PLX4032 exerted little or no changes.

Figure 6

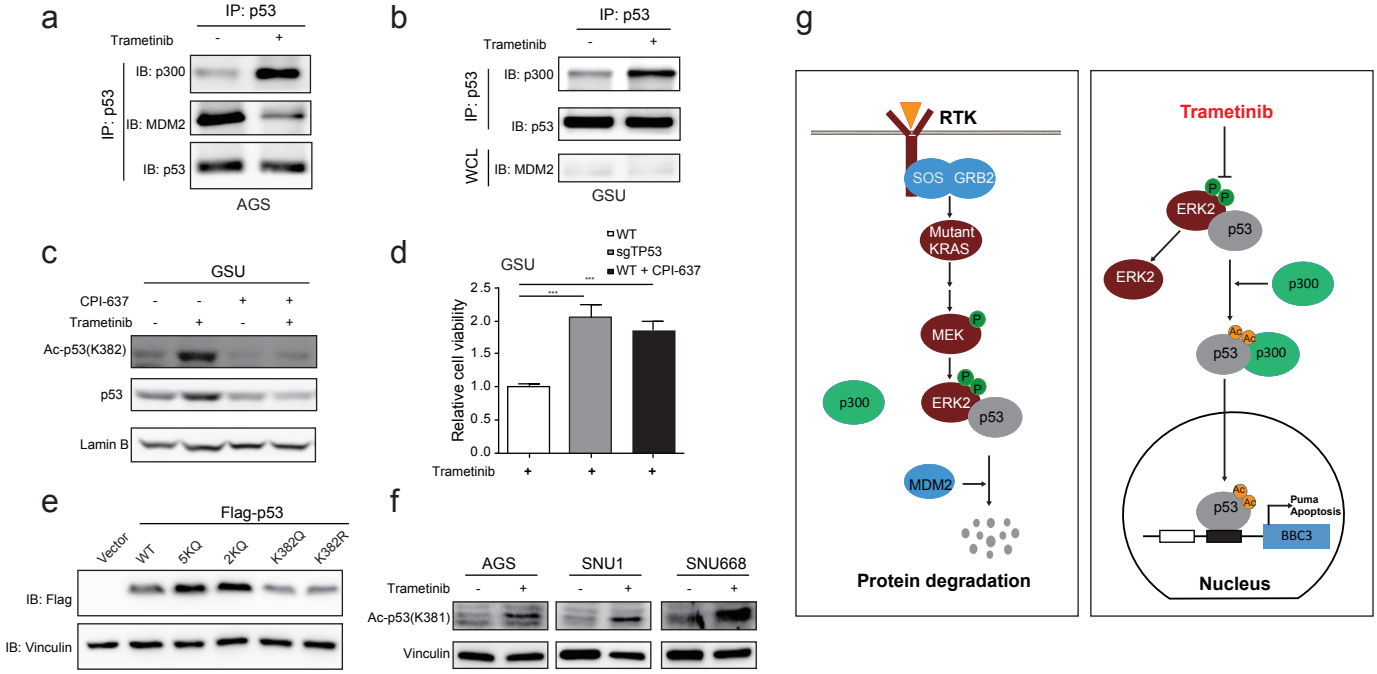

Figure 6. Trametinib promotes p53 acetylation by recruiting p300/CBP. (a) Trametinib robustly increased the physical association between p53 and p300 in KRAS-mutant AGS cells after treatment for 12 hours. The binding of p53 to MDM2 was decreased after trametinib treatment. (b) Treatment with trametinib for 4 hours robustly increased the physical association between p53 and p300 in KRAS-mutant GSU cells. There was little or no MDM2 protein expression in GSU cells. (c) The p300/CPB inhibitor CPI-637 significantly reduced the levels of K382-acetylated and total p53 protein. (d) CPI-637 robustly rescued the viability of KRAS-mutant GSU cells upon trametinib treatment. (e) p53 5KQ and 2KQ mutants but not the K382Q mutant had better protein stability than wild-type. (f) Trametinib increased the acetylation of p53 protein at lysine 381 in multiple KRAS-mutant cell lines. (g) A cartoon of our working model.